J. CHEM. SOC. FARADAY TRANS., 1992, 88(22), 3331–3337

Thermodynamic Studies of Gas-phase Proton Transfer Equilibria involving Benzene: A Reassessment of Earlier Data†

Alyn Parry,‡ M. Tereza Fernandez,¶ Mike Garley and Rod Mason*
Department of Chemistry, University College of Swansea, Singleton Park, Swansea SA2 8PP, UK

Temperature-variable equilibrium constant measurements have been performed for a number of proton-transfer equilibria in which benzene was a partner, using a newly built high-pressure pulsed source mass spectrometer. Entropy values obtained showed that the protons in protonated benzene are not as mobile as previously thought. Systems involving ethanol are found to give anomalous, though self-consistent results owing to the onset of thermal decomposition. In the light of this, previous data involving halotoluenes and xylenes which appear to show unusually large increases in entropy on protonation, have been reassessed. There is evidence of proton-induced isomerisation. In the reaction $[4\text{-}ClC_6H_4CH_3]H^+ \rightarrow [3\text{-}ClC_6H_4CH_3]H^+$ the free energy of activation is derived to be *ca.* 90 kJ mol^{-1} from a computer model fit to the results, consistent with the energy calculated to be needed for a proton shift from the 3 to the 4 position in the precursor. The equivalent reaction for protonated 4-fluorotoluene has a barrier which is *ca.* 10 kJ mol^{-1} higher. A kinetic scheme is presented which shows how this could account for the observed 'thermodynamic' behaviour, and also give rise to the 'isokinetic effects' previously noted. There has therefore been some readjustment of the recommended proton affinity values for some of these compounds.

Thermodynamic studies of gas-phase reactions by a variety of techniques are well established.[1] The most easily and comprehensively studied systems have been those involving proton-transfer equilibria (I).[2]

$$AH^+ + B = A + BH^+ \quad (I)$$

The data obtained are very useful as a source of thermodynamic data in mechanistic studies and for elucidating structure–reactivity relationships in the absence of solvent effects.[1,3] Proton affinities (P_A), defined as the enthalpy (ΔH°) of reaction (II),

$$AH^+ \rightarrow A + H^+ \quad (II)$$

are measured relative to each other from the temperature dependence of the equilibrium constant (K_{eq}) using the classical relationships (1) and (2), where ΔS_1° is the change in entropy at the temperature T.

$$\Delta G_1^\circ = \Delta H_1^\circ - T\Delta S_1^\circ \quad (1)$$

$$\Delta H_1^\circ = P_A(A) - P_A(B) \quad (2)$$

In most cases ΔS_1° values are negligible owing to cancellation effects, except where there are changes in rotational symmetry or 'internal rotations'.[4] The value of the former can be predicted using the relationship derived from statistical mechanics:

$$\Delta S = \Delta S_{rot} = R \ln\left(\frac{\sigma_{AH}^+ \cdot \sigma_B}{\sigma_{BH}^+ \cdot \sigma_A}\right) \quad (3)$$

This approximation holds for the majority of simple proton-transfer reactions but is found to break down when structure changes on protonation lead to a locking (or indeed a release) of rotational and/or vibrational modes,[5] when experimental verification is necessary.

Recently, anomalous behaviour was observed[6] in experiments involving 1,2- and 1,4-disubstituted aromatic compounds where the extra proton sits on the ring carbon atoms. It is well known that the protons in protonated aromatic compounds can be extremely mobile because of the low barriers to 1,2-migration around the ring carbon atom.[7] In the previous work it was noted[6] that systems involving halotoluenes and xylenes, particularly the 4- and to a lesser extent the 2-substituted compounds exhibited very large apparent increases in entropy upon protonation. This gave rise to the interesting though controversial, idea, of entropy contributions due to the 'free movement' of the proton around the ring,[7] in a manner analogous to the free internal rotation concept which also gives rise to significant increases in entropy. However, for this to happen at experimentally accessible temperatures ($300 < T/K < 650$) energy barriers would need to be <20 kJ mol^{-1}, whereas molecular orbital (MO) calculations on benzene itself indicate the barrier to 1,2 proton migration to be in the region of 30–40 kJ mol^{-1}, too high to show an effect.[7]

Much earlier temperature dependence studies of proton transfer involving benzene had demonstrated only small changes in entropy.[8] However, since the partners in these studies were also both aromatic and ring protonating, the possibility occurs of excess entropy contributions being masked by cancellation effects.

In this paper we report the results of a study to measure the entropy of protonation of benzene relative to non-aromatic compounds (and hence avoid any possibility of cancellation effects) using a recently constructed high-pressure pulsed source (HPPS) mass spectrometer system, which is also described. The systems involving the halotoluenes are also re-examined, as is the reaction between the halotoluenes and benzene.

During the preparation of this manuscript a detailed general study of the temperature dependence of many proton-transfer equilibria has appeared in the literature[9] with the aim of searching for other 'dynamically' protonated molecules, but without success. Two of the systems studied here ($C_6H_7^+$–CH_3OH and $C_6H_7^+$–CH_3CHO) were included in that study.

† This work was first reported at the 25th meeting of the British Mass Spectrometry Society, London, 1990. A. Parry, Ph.D. Thesis, University College Swansea, 1991.

‡ Present address: Unilever Research, Port Sunlight Laboratory, Quarry Road East, Bebington, Wirral L63 3JW, UK.

¶ Permanent address: Centro de Expectromeria de Massa, Instituto Nacional de Investigacao Cientifica, Instituto Superior Tecnico, Av. Rovisco Pais 1, 1096 Lisboa Codex, Portugal.

Apparatus and Method

The experiments were performed using a new pulsed electron beam high-pressure ion source, constructed in-house, and coupled to an updated (by MSS Ltd., Manchester, UK) MS9 mass spectrometer system. The source, coaxial in design, is shown in Fig. 1–3.

The electron gun mounted onto the source assembly base plate has a conventional heated filament separated by 14 mm from the main source block. Two 2 mm aperture plates in between serve three functions: to stabilise emission from the filament, focus the electron beam and to switch it on and off when required. The emission from the filament reaching the first plate is fed back *via* a small isolation amplifier chip to the filament current control circuit, and maintains a constant emission even in the pulsed mode. Scatter in the data was considerably reduced when this facility was used. When switched into pulsed mode the second plate is biased 13 V negative with respect to the filament, completely repelling the electron beam, provided the positive bias on the first plate is <15 V. A square wave positive-going pulse momentarily supplies a positive bias of 13 V onto the second plate for a selected time period, usually between 1 and 100 μs, allowing a pulse of ionising electrons (usual energy 100–400 eV†) to penetrate the reactant gas in the ion source through a 0.3 mm diameter aperture.

The control pulses are provided by a dual pulse generator (Lyons Instruments, PG71N Bipolar), from which one pulse is used to trigger the multichannel analyser data collection and averaging system. The second pulse, delayed by 1 ms, triggers a second pulse generator (Thurlby-Thander, TG105, from Radio Spares). This controls the pulsing of the electron beam. The 10 V output pulse fires an LED, the light pulse passing down a fibre-optic cable to a pulse converter close to the ion source and floating at the potential of the second focus plate. By making use of the 'complement' button on the TG105 it was possible to switch readily between continuous-mode operation for tuning up and recording chemical ionisation (CI) spectra and pulsed mode for the equilibrium measurements.

The ion chamber itself is cylindrical with a diameter and length each of 10 mm. The surrounding cylindrically shaped stainless-steel block (60 mm diameter × 18 mm deep) is mounted onto the base plate by 19 mm stainless-steel pillars.

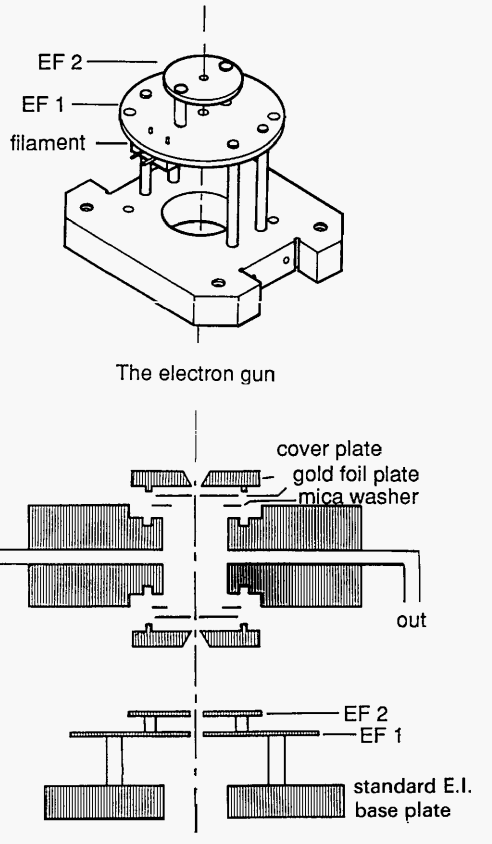

Fig. 2 (*a*) The electron beam assembly; (*b*) section through the source block showing electron entrance and ion exit plates, stainless-steel cover plates and source chamber in relation to the electron gun

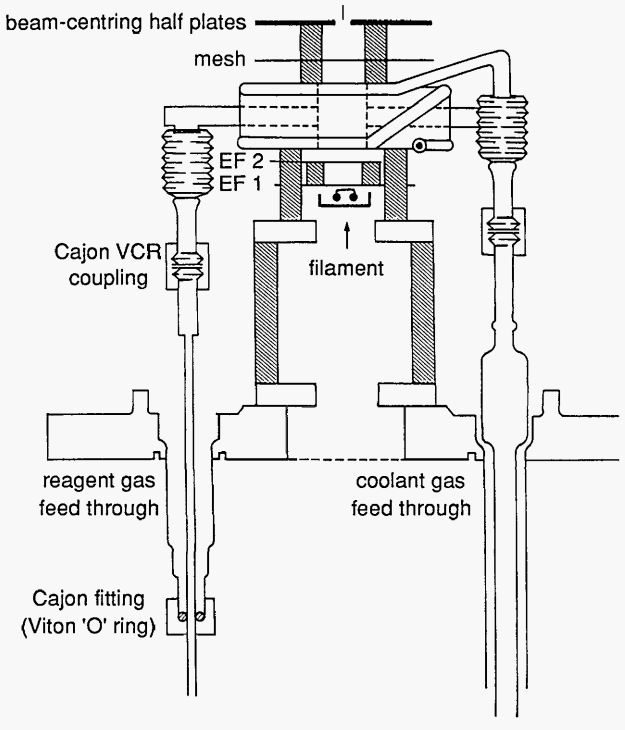

Fig. 1 **Schematic of the** pulsed high-pressure source mounted on the source housing flange

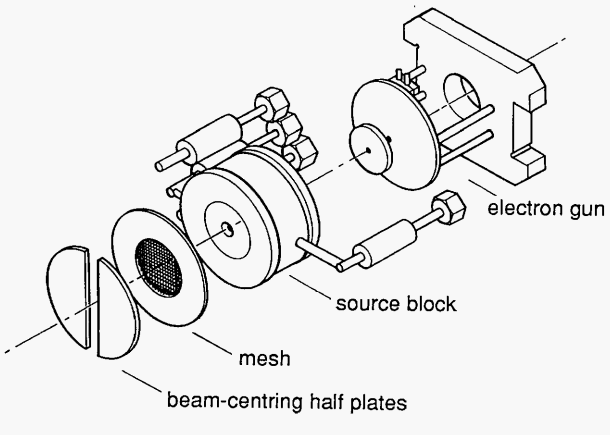

Fig. 3 Exploded view of the pulsed high-pressure source

† 1 eV ≈ 1.602×10^{-19} J.

Heaters, 6 cm long, were constructed by passing a 0.007 in. tungsten wire six times through a 2 mm diameter ceramic former, which itself fits into and through clearance holes in the block. Two such heaters in series enable heating of the block to temperatures >400 °C, though the wire becomes brittle after use. A hollow tube wrapped twice around the block and connected *via* ceramic insulating feedthroughs to a cooled flow of N_2 gas enables cooling to < −100 °C. The temperature is measured using a ceramic-encapsulated Pt resistance thermometer (20 × 1.5 mm) inserted into the block close to the ion chamber.

The ion chamber is sealed at each end by gold foil (Goodfellow Metals, 99.5% purity, pinhole-free) discs (0.025 mm thick) clamped to the block by a stainless-steel plate. 0.3 mm diameter holes in the centre of the discs served as electron entrance and ion exit apertures. All the inner surfaces were coated with colloidal graphite (baked on at 200 °C under vacuum overnight) to suppress the build-up of non-conducting surface layers, as reported before.[10]

The ion focus and beam centring plates were mounted onto the source block 10 and 21 mm from the ion exit, respectively. The whole assembly was mounted onto quartz plates which were bolted to the source housing flange in the usual way. Electrical and gas supplies pass *via* electrically insulated feedthroughs through this flange (similar to the ion–molecule reactor previously built for this type of mass spectrometer).[6,10] When in position the beam-centring plates are 10 mm from the adjustable source slit at the entrance to the mass spectrometer. The source housing was differentially pumped by a 600 $dm^3\ s^{-1}$ diffusion pump (Edwards, type 180-700).

A pressure transducer (Baratron), to measure the pressure inside the ion chamber, and automatic inlet and pressure control valve (MKS type 248A), both connected to the ion chamber by *ca.* 30 cm lengths of 3 mm tubing, were housed in a heat insulated Teflon box sitting on top of a heated oven containing the gas storage and manifold. The valve and transducer were kept at *ca.* 50 °C by hot air blown through from the oven.

The pressure control and readout, temperature control and readout, gate pulse converter and amplifier were all housed in a Perspex box close to the source housing and floated at the operating voltage of the ion source making use of a mains-voltage isolation transformer.

Ion beam signals were detected using a single-channel electron multiplier (SCEM, Phillips X919AL) and Cu–Be front dynode conversion plate arrangement, described previously.[11] In continuous mode, the SCEM is operated at low gain and the current detected using the standard mass spectrometer console and UV oscillograph for recording mass spectra. In pulsed mode the mass spectrometer is focused on one mass peak at a time. The SCEM is operated at high gain (1×10^8) and the signal is passed through a fast amplifier for detection by a 'single-ion' counting system (EG&G). Time-dependent signals are accumulated on a multichannel analyser (EG&G, Ortec-Norland 5600), dwell time: 10 μs per channel, scanning through 10 ms after the ionising electron pulse, thus generating a reaction–time profile for the chosen mass peak. Averaging by summing over (10–50) × 10^3 sweeps was required to achieve satisfactory signal-to-noise ratios in the late part of the time profile where the ions in the chamber have had time to become thermalised and the ion density has become low enough to allow free diffusion.

All reagents used in this work were commercially available with purity >99%. Any impurities present did not show up in the chemical ionisation mass spectra, the compounds were therefore used without further purification. Accurate mixtures of the pairs of neutrals were made up by weighing. Aliquots of between 1 and 50 mm^3 were injected through a septum inlet into the 4 dm^3 glass bulb heated to *ca.* 120 °C, containing typically 1000 mbar of methane (BOC Research Grade).

The principles of the method and the manner of generating equilibrium constants are well documented in the literature.[12] The equilibrium constant in reaction (I), given by

$$K_1 = \frac{[A][BH^+]}{[B][AH^+]} \quad (4)$$

is determined from the ratio of intensities of the pair of ions, obtained in the free-diffusion region of the afterpulse, multiplied by the premixed molar ratio of the pair of neutrals. Checks on the integrity of the equilibrium (or steady-state) data at a specific temperature were made by varying the reaction conditions (total and partial pressures).

Results

The set of proton-transfer equilibria studied in this work is shown in Table 1. The non-aromatic compounds in the benzene region of the proton affinity scale tend to be quite polar. A problem, endemic with all such compounds, is their tendency to form proton-bound ion–molecule clusters or adducts which may interfere with the equilibrium measurement.[13] The problem is usually circumvented by choosing a suitable range of experimental conditions, since clustering

Table 1 Summary of results

system	A	B	T_{range}/K	[A]/[B][a]	no. of data points	$-\Delta H^\circ_{expt}$ [b]	$-\Delta H^\circ_{lit}$ [c]	$-\Delta S^\circ_{expt}$	$-\Delta S^\circ_{rot}$ [d]
III	C_6H_6	C_6H_5F	350–550	1.0	21	5.8 ± 0.4	5.4	14.9 ± 0.9	14.9
IV	C_6H_6	CH_3OH	530–645	0.3–0.7	38	3 ± 2	2	18 ± 4	14.9
V	C_6H_6	CH_3CHO	530–644	4.55	21	19 ± 2	22	21 ± 3	14.9
VI	C_6H_6	C_2H_5OH	490–620	9–23	76	55 ± 2	29	83 ± 4	
			490–540			24 ± 6		23 ± 11	14.9
VII	CH_3CHO	C_2H_5OH	530–620	1.4	20	30 ± 5	7	46 ± 8	
			530			(5.3 ± 1.7)		(0)	0
VIII	CH_3OH	CH_3CHO	530–640	2.9–4.3	44	16 ± 4	20	5 ± 6	0
IX	C_6H_6	4-$CH_3C_6H_5F$	293–390	9–25	14	20 ± 2	4	36 ± 4	9.1–14.9
X	C_6H_6	4-$CH_3C_6H_5Cl$	313–380	2.4–25.5	8	15 ± 5		23 ± 13	9.1–14.9
XI	4-$CH_3C_6H_5F$	4-$CH_3C_6H_5Cl$	295–393	1.0	12	3.9 ± 0.8	−1.2	12 ± 3	0

[a] Range of neutral concentration ratios studied. [b] All ΔH° values are in units of kJ mol^{-1}; ΔS° values are in J mol^{-1}. [c] Values calculated from table of proton affinity values published in ref. 17. [d] Calculated from changes in rotational symmetry using eqn. (3); $\sigma_{benzene} = 12$, all other neutral or protonated species have a σ value of either 1 or 2. [e] Steady state not reached above *ca.* 410 K.

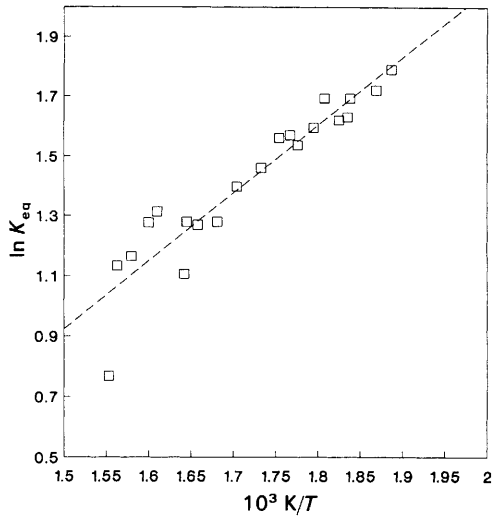

Fig. 4 Van't Hoff plot of data from reaction (V),

$$C_6H_7^+ + CH_3CHO \rightleftharpoons C_6H_6 + CH_3CHOH^+$$

usually obeys third-order kinetics with a negative temperature coefficient. Therefore the effect is reduced by operating at either lower pressures and/or higher temperatures. It is for this reason that most HPPS data are quoted at 600 K. The molecules paired with benzene here [reactions (IV)–(VIII)] were chosen as the least polar of those with suitably matched proton affinities. The lower-temperature limit for measurement had to be set at 450 K. This was checked by ensuring that the intensities of all cluster ions present in the afterpulse time profile were always <10% of the lowest abundance ion of interest. The pressure of the methane bath gas was usually in the region of 2–4 Torr† and partial pressures of the neutrals were in the region of (10–100) × 10^{-5} Torr.

For all the reactions, the temperature dependences of K_{eq} were obtained as a function of both pressure and neutral concentration ratio, to establish that values did not vary outside the limits of reproducibility. An indication of the degree of scatter is shown in Fig. 4 for reaction (V). When straight-line plots of ln K_{eq} against $1/T$ were obtained, values of $\Delta H°$ and $\Delta S°$ were derived. The results are detailed in Table 1, and displayed in the form of thermodynamic ladders in Fig. 5. Within the margin of experimental error, overlapping thermodynamic values are seen to be self-consistent.

Reaction (III) was studied first because it has been examined several times before in different laboratories on instruments of different source geometries and its temperature dependence is therefore well characterised.[14] The results obtained are in exact agreement showing the new source to be equally capable of studying thermal equilibria. Reactions (IX) and (XI) have also been studied before[6] but not over the relatively low temperature range covered here.

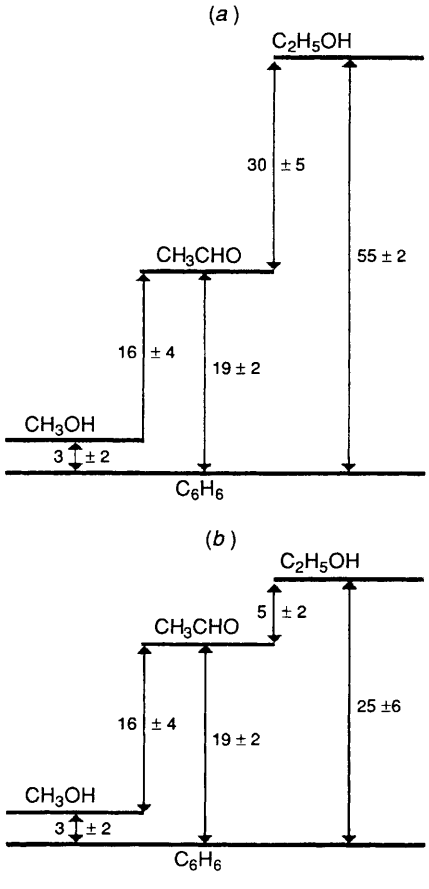

Fig. 5 Ladder showing relative enthalpy changes for reactions (IV)–(VIII); (*a*) over the full temperature range explored; (*b*) discounting the higher-temperature data for reactions involving C_2H_5OH

Discussion

The data obtained are thermodynamically self-consistent within the limits of error. This type of self-consistency is usually a good test of the integrity of the thermodynamic data (based on a very large number of similar equilibrium experiments in the past).[9,12] Nevertheless, the measured 'apparent' entropy changes recorded in Table 1 highlight an interesting anomaly. The benzene–ethanol system (VI) appears to show the large entropy change in favour of protonated benzene as might be expected if protonated benzene has a dynamic structure (discussed in the Introduction). However, the benzene–methanol (IV) and benzene–ethanal (V) systems both give values close to those predicted on the basis of their rotational symmetries. This implies that it is the ethanol that is anomalous. This is confirmed by the apparent $\Delta S°$ value for the ethanal–ethanol system which if true would indicate that ethanol is actually losing a significant degree of entropy on protonation. This cannot be correct, since theoretical computation shows the lowest-energy structure of protonated ethanol to be **1**. The energies of different rotational conformers, **1**, **2** and **3**, are close, with the barrier calculated as being 6 kJ mol^{-1} (relative energies for each of the protonated rotational conformers were calculated by semi-empirical molecular orbital theory using the MNDO QCPE package). If anything, we would expect a slight increase after protonation on the oxygen caused by a probable slight increase in the degree of 'internal rotation'.

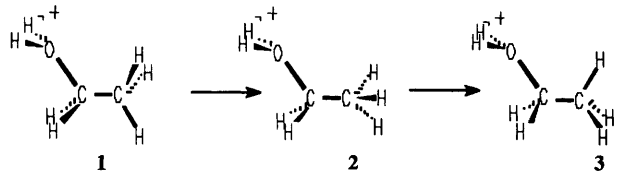

1 **2** **3**

As reported elsewhere,[15] closer examination of the ethanol data reveals a pronounced curvature in the plot of $\Delta G°$ *vs.* T.

† 1 Torr = (101 325)/760 Pa.

It was shown that this behaviour is caused by catalytic cracking of the ethanol on the hot surface of the ion source at high temperatures, leading to erroneous values of K^{VI} which remain consistent even with changes in total and partial pressures. Meot-Ner and Sieck report[9] observation of anomalous entropy changes in charge- and proton-transfer systems which can be ascribed to decomposition or isomerisation reactions; this can usually be identified if it leads to inconsistency in the overlapping thermodynamic cycles. The measurements recorded here, however, show that thermodynamic self-consistency can still appear to be maintained, even though decomposition may occur.

Ethanol pyrolysis was found not to be significant at temperatures <540 K in our apparatus.[15] Although this is close to the lower-temperature limit before ethanol dimerisation becomes significant, the data in the interval 490–540 K have been used to estimate the proton affinity of ethanol as 24 ± 6 kJ mol^{-1} relative to benzene. This puts $P_A(C_2H_5OH)$ at 783 ± 6 kJ mol^{-1}, similar to that deduced by Kebarle *et al.*[16] based on free energy measurements at 600 K, but lower than the value recommended in Lias *et al.*'s compilation.[17] In the ethanol–ethanal system (VII) the practical lower-temperature limit was higher, *ca.* 520 K, because of the increased probability for mixed cluster formation. However, the data in the 530 K region yields a ΔG^{532} value of 5.3 ± 1.7 kJ mol^{-1} in favour of protonated ethanol. This is consistent with the proton affinity of acetaldehyde measured in system (V) to be $19 + 2$ kJ mol^{-1} greater than benzene. This in turn is in excellent agreement with the value obtained by Meot-Ner and Sieck.[9] The P_A value for ethanol is therefore 8–10 kJ mol^{-1} below that recommended previously.[17]

With regard to benzene, therefore, this work confirms that upon protonation there is no significant entropy change beyond that expected from rotational symmetry changes (and again is in agreement with the recent work of Meot-Ner and Sieck) even though the protons are known to be highly mobile.[7] This is to be expected if the 1,2 proton migration barrier height is 30–40 kJ mol^{-1}. With this barrier, proton migration rates are expected to be in the region of 10^9 s^{-1}, as occurs in the liquid phase,[18] and therefore are too slow to affect the entropy. Taking a different approach, Attina *et al.*[19] have recently used kinetic arguments based on the analysis of radiolysis products in mixtures of C_3H_8-containing substituted aromatics to deduce that the rate of proton migration in $C_6H_7^+$ is indeed probably of the order of 10^9 s^{-1} in the gas phase.

The anomalously large entropy changes previously measured[6] for the 4- and 2-substituted fluoro- and chlorotoluenes are now brought into question. How do they compare when measured against benzene? Though not investigated in any depth, anomalous behaviour was already noticed in the previous experiments[7] when 4-fluorotoluene was paired with benzene. It was noted that the van't Hoff plot showed a sudden apparent change in slope, in favour of the protonated fluorotoluene at temperatures >450 K. The experiment was explored further here [system (IX)]. The system behaved normally up to 410 K (see Fig. 6) with the higher energy species, protonated benzene, becoming more favoured at higher temperatures as expected on thermodynamic grounds. Above this temperature, the system began to favour the protonated halotoluene more with increasing T, rapidly reaching a stage where equilibrium could not be achieved. Investigation here of the benzene–4-chlorotoluene system (X) shows the van't Hoff plot to behave in a similar manner (see Fig. 7). No such behaviour had been evident in the previous work involving halotoluene pairs.[6]

Careful examination of the mass spectra from the reaction mix, both in the continuous and pulsed modes, indicated that

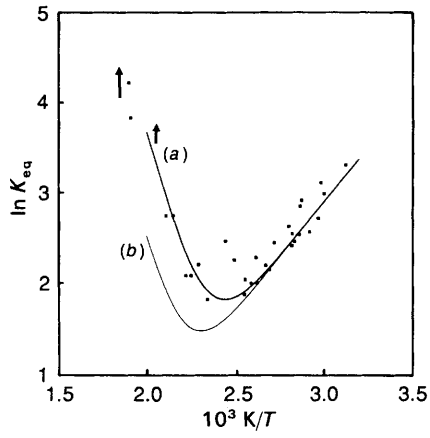

Fig. 6 Reaction (IX): $C_6H_6^+ + 1,4\text{-}CH_3C_6H_4F \rightleftharpoons C_6H_6 + 1,4\text{-}CH_3C_6H_4FH^+$; ln K_{app} *vs.* $1/T$; □, exptl. data; ——, variation according to the computer model (Scheme 1), in which $\Delta H°$ for reactions (a), (d') and (e') = −20, −14 and −34 kJ mol^{-1}, respectively, and $\Delta G^{\#} = 85$ (*a*) or 90 kJ mol^{-1} (*b*)

there are no new product ions involved. The only rational explanation for such a result is that the protonated 4-substituted compounds isomerise at the higher temperatures to a new species from which back transfer of the proton to benzene has a much lower probability. This newly formed species is almost certainly the protonated 3-compound. Transfer of the proton back from this species will be very much slower, because it has a significantly higher proton affinity than the 1,4-isomer. The behaviour for both fluoro and chloro compounds is observed to be almost identical, so that when paired together in proton-transfer equilibrium the effect is much less apparent.

Scheme 1 shows the complete series of reactions that are assumed to be occurring in the late afterglow of system (IX) at these higher temperatures.

$$BH^+ + pFT \rightarrow B + pFTH^+ \quad \text{(a)}$$

$$pFTH^+ + B \rightarrow pFT + BH^+ \quad \text{(b)}$$

$$pFTH^+ \rightarrow mFTH^+ \quad \text{(c)}$$

$$mFTH^+ + pFT \rightarrow mFT + pFTH^+ \quad \text{(d)}$$

$$mFTH^+ + B \rightarrow mFT + BH^+ \quad \text{(e)}$$

$$\left.\begin{matrix} BH^+ \\ pFTH^+ \\ mFTH^+ \end{matrix}\right\} \rightarrow \left\{\begin{matrix}\text{diffusive loss to walls} \\ \text{of reaction chamber}\end{matrix}\right\} \quad \text{(f)}$$

Scheme 1 B = benzene; *p* and *m*FT = *para* (4-) and *meta* (3-) fluorotoluene

The exothermic (forward) proton-transfer rate constants (k_a, k'_d and k'_e) can be calculated using 'ADO' theory.[20] The endothermic (backward) proton-transfer rate constants (k_b, k_d and k_e) can be calculated using the relationships:

$$K_{eq} = k_{forward}/k_{back}; \quad k_{back} = k_{forward} \exp(\Delta G°/RT)$$

where the tabulated or measured values of $\Delta H°$ and $\Delta S°$ are used to determine $\Delta G°$. The diffusive-loss rate coefficient (k_f) was determined as a function of temperature from the recorded time profiles, as before.[10] The value of k_c was assumed to have the conventional transition-state theory form: $k_c = (kT/h)\exp(-\Delta G^{\#}/RT)$, where k and h are Boltzmann's and Planck's constants and $\Delta G^{\#}$ is the free energy of activation, the only unknown. Using trial values of $\Delta G^{\#}$ and the calculated rate constant values we were able to simulate the reaction by computer integration of the rate equations.

The results shown in Fig. 6 and 7 fit well with the experi-

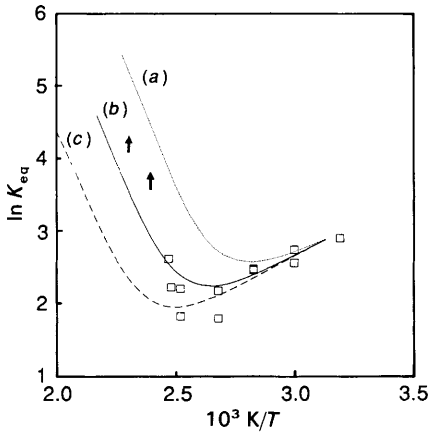

Fig. 7 Reaction (X): $C_6H_6^+ + 1,4\text{-}CH_3C_6H_4Cl \rightleftharpoons C_6H_6 + 1,4\text{-}CH_3C_6H_4ClH^+$; ln K_{app} *vs.* $1/T$; □, exptl. data; · · ·, – – –, ——, variation according to the computer model (scheme 1), in which $\Delta H°$ for reactions (a), (d′) and (e′) = −15, −20 and −33 kJ mol^{-1}, respectively, and $\Delta G^{\#}$ = 75 (*a*), 80 (*b*) or 85 kJ mol^{-1} (*c*)

mental data when $\Delta G^{\#}$ has a value between 90 and 95 kJ mol^{-1} for protonated 4-fluorotoluene, and 80–83 kJ mol^{-1} for 4-chlorotoluene. These are probably upper-limit values because the calculated rate constants (k_a, k'_d and k'_e) are upper-limit values. If these are deliberately reduced by a factor of 10, the predicted $\Delta G^{\#}$ values are also lowered by 10 kJ mol^{-1}. In addition, the transition-state theory expression is valid, strictly speaking, only at the high-pressure limit, which is probably not reached at our experimental pressures, again tending to an overestimation of $\Delta G^{\#}$.

The proton-induced isomerisation process requires a 1,2 migration of either the halogen or the methyl group, presumably induced by the proton becoming attached at the carbon atom *ipso* to the substituent. Two pieces of evidence point to migration of the halogen being the dominant process. The first is that the protonated xylenes paired against dimethyl ether at high temperatures do not show any dramatic effects.[21] The second is that whereas the proton bound to the carbon *ipso* to the methyl group is a low-energy species, the proton bound *ipso* to the halogen is not.[22] Indeed, the value of $\Delta G^{\#}$ derived above is consistent with the energy difference, determined[22] using MO theory to be 108 kJ mol^{-1}, between the molecule protonated on the carbon *ipso* to the halogen and the molecule protonated at the other carbon atoms of the ring. The circumstantial evidence is therefore consistent with migration of the proton to the *ipso* position as being the probable rate-determining step of this thermal isomerisation reaction.

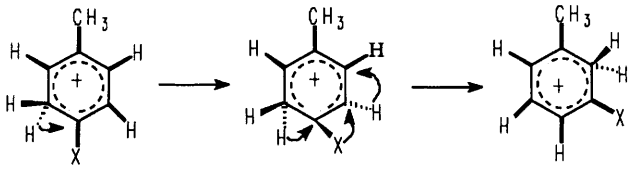

Thermal Isomerisation of Protonated *para*-Halotoluenes

For systems (IX) and (X), therefore, there is an upper temperature limit of 380 and 410 K, respectively, for the equilibrium experiments beyond which isomerisation becomes significant. Analysis of the lower-temperature data (Table 1) still shows a relatively large entropy change, but indicating a decrease (opposite to that which is expected on the basis of the previous work)[6] when the proton is transferred to the 4-substituted halotoluenes from benzene.

The halotoluene systems were previously studied in the temperature region 385–600 K where the isomerisation reaction is now thought to be significant. If, for the sake of simplicity, we assume that only one of the pair undergoes isomerisation (though both may actually do so) then a simple reaction sequence can be inferred as represented in Scheme 2. Here one of the participants, AH^+, of reaction (a) isomerises in (b) to the lower-energy species, $A'H^+$, which in order to maintain a pseudo-steady state must continue to participate in proton-transfer reactions back to form AH^+ and BH^+, though at a lower rate than the back reaction (−a) because of the greater difference in proton affinities. Diffusion is the ultimate loss process but diffusion rates are very slow compared with proton transfer and equal for each ion of the pair (thus cancelling out in the final analysis); they are therefore ignored.

$$AH^+ + B \rightleftharpoons A + BH^+ \quad \text{(a, −a)}$$

$$AH^+ \rightarrow A'H^+ \quad \text{(b)}$$

$$A'H^+ + A \rightarrow A' + AH^+ \quad \text{(c)}$$

$$A'H^+ + B \rightarrow A' + BH^+ \quad \text{(d)}$$

Scheme 2

In the mass spectrometer AH^+ and $A'H^+$ are indistinguishable because their masses are identical. Overall, experimentally, AH^+ and $A'H^+$ decay at the same rate as BH^+; therefore

$$d[AH^+]/dt + d[A'H^+]/dt = d[BH^+]/dt$$

and the following relation can be derived using the normal kinetic rules:

$$k_{-a}[BH^+][A] = (k_a[AH^+] + k_d[A'H^+])[B] \quad (5)$$

which rearranges to give eqn. (6)

$$K_{app} = K_a(x + yk_d/k_a) \quad (6)$$

where $K_{app} = [A][BH^+]/\{[B]([AH^+] + [A'H^+])\}$, which is the quantity experimentally measured; $K_a = [A][BH^+]/[B][AH^+]$, the true thermodynamic equilibrium constant; $x = [AH^+]/([AH^+] + [A'H^+])$; $y = [A'H^+]/([AH^+] + [A'H^+])$ and k_d and k_a are rate constants. Reaction (d) is endothermic and k_d is therefore assumed equal to $k_a \exp(-\Delta G°_{d'}/RT)$, where $\Delta G°_{d'}$ is the free energy change in the exothermic direction (when the rate is assumed equal to the ADO collision frequency as before, hence $k_{d'} = k_a$). The apparent equilibrium constant is then given by:

$$K_{app} = K_a(x + y/K_{d'}) \quad (7)$$

where K_a is the true equilibrium constant, and $k_{d'}$ the thermodynamic constant for proton transfer to the lower energy isomer, reaction (d′),

$$BH^+ + A' \rightleftharpoons BH + A'H^+ \quad \text{(d′)}$$

$K_{d'} > 1$, because the proton affinity of A′ is greater than that of B in the halotoluene systems. As the temperature increases, y increases because of isomerisation at the expense of x, so decreasing the value of K_{app} relative to K_a. This will have the effect of increasing the slope and hence decreasing the intercept of the van't Hoff plot as is observed experimentally, hence giving artefact values for $-\Delta H°$ and $\Delta S°$. In these circumstances the changes will be directly proportionate and could therefore give rise to an apparent correlation between $\Delta H°$ and $\Delta S°$ as was previously observed.[6] Such correlations are probably the origin of the isokinetic relationships. The existence of such relationships has been the subject of con-

Table 2 Proton affinities[a] (P_A/kJ mol^{-1}) of the fluoro- and chlorotoluenes ($CH_3C_6H_5X$)

3-isomer		2-isomer		4-isomer	
F	Cl	F	Cl	F	Cl
792 ± 1	791 ± 1	781–785	779–783	776 ± 3	772 ± 3

[a] Determined from the equilibrium constant data at ⩽380 K in ref. 6, re-evaluated ΔH° values for systems (IX)–(XI) in Table 1 and using, as anchor points, the recommended[19] P_A values for benzene and toluene at 759 and 794 kJ mol^{-1}, respectively.

siderable argument in the past[23] when antagonists argued that they are likely to be the result of an artefact, as finally proves to be the case in these gas-phase systems.

We must conclude, therefore, that at higher temperatures it is probably the thermal isomerisation of protonated 2- and 4-halotoluenes that is responsible for their anomalous thermochemical behaviour. Because of the effects noted here, the P_A values for some of the species studied are different from those previously recommended. These revised values based on the low-temperature data alone are summarised in Table 2.

Proton transfer to the xylenes causes similar effects,[21] though at a reduced level compared with the halotoluenes. Again, it is the protonated 3-substituted compound that is most stable. In this case, acid-catalysed isomerisation has been observed in super-acid solution,[24] in which the 4-substituted compound was converted to the 3- slightly more readily than the 2-compound. Measured against diethyl ether in the gas phase, the effects were less dramatic even though the temperature range of 573–725 K was significantly higher than that employed for the halotoluene–benzene systems. In the case of the xylenes, of course, isomerisation can occur only by migration of a methyl group, presumably with a considerably higher energy of activation. In the same way, a high entropy change noted[25] in the 1,2-dichlorobenzene–1,3,5-trifluorobenzene system could also be explained by proton-induced isomerisation to the more stable[14a] 1,2,5-trifluorobenzene isomer.

We thank the SERC for an Earmarked studentship (A.P.), and the Gulbenkian Foundation for financial support (M.T.F.). We are also most grateful to Des Thomas of The Mass Spectrometry Research Unit, University College Swansea, for his outstanding skills in mechanical engineering during the building of this instrument and for his continuing technical support.

References

1 M. T. Bowers (Ed.), *Gas Phase Ion Chemistry*, Academic Press, New York, 1979, vol. 1 and 2.
2 J. E. Bartmess, *Mass Spectrom. Rev.*, 1989, **8**, 297.
3 R. W. Taft, in *Kinetics of Ion–Molecule Reactions*, ed. P. Ausloos, Plenum Press, New York, 1979, NATO ASI Series B, p. 271.
4 S. G. Lias, in ref 3, p. 224.
5 R. Yamdagni and P. Kebarle, *J. Am. Chem. Soc.*, 1973, **95**, 3504.
6 M. T. Fernandez, K. R. Jennings and R. S. Mason, *J. Chem. Soc., Faraday Trans. 2*, 1987, **83**, 159.
7 R. S. Mason, M. T. Fernandez and K. R. Jennings, *J. Chem. Soc., Faraday Trans. 2*, 1987, **83**, 89.
8 Y. K. Lau and P. Kebarle, *J. Am. Chem. Soc.*, 1976, **98**, 7452.
9 M. Meot-Ner and L. W. Sieck, *J. Am. Chem. Soc.*, 1991, **113**, 4448.
10 J. V. Headley, R. S. Mason and K. R. Jennings, *J. Chem. Soc., Faraday Trans. 1*, 1982, **78**, 933.
11 A. Parry and R. S. Mason, *Adv. Mass Spectrom.*, 1989, **11**, 214.
12 P. Kebarle, in *Techniques in Chemistry*, ed. J. M. Farrar Jr. and W. H. Saunders, Wiley, New York, 1988, vol. 20.
13 D. H. Aue and M. T. Bowers, in *Gas Phase Ion Chemistry*, ed. M. T. Bowers, Academic Press, New York, 1979, vol. 2, ch. 9.
14 (*a*) K. G. Hartmann and S. G. Lias, *Int. J. Mass Spectrom. Ion Phys.*, 1978, **28**, 213; (*b*) D. K. Bohme, J. A. Stone, R. S. Mason, R. S. Stradling and K. R. Jennings, *Int. J. Mass Spectrom. Ion Phys.*, 1981, **37**, 283.
15 R. S. Mason and A. Parry, *Int. J. Mass Spectrom. Ion Phys.*, 1991, **108**, 241.
16 P. Kebarle, R. Yamdagni, K. Hiraoka and T. B. McMahon, *Int. J. Mass Spectrom. Ion Phys.*, 1976, **71**, 16.
17 S. G. Lias, J. E. Bartmess, J. F. Liebmann, J. L. Holmes, R. D. Levin and W. G. Mallard, *J. Phys. Chem. Ref. Data*, 1988, vol. 17.
18 G. A. Olah, R. H. Schlosberg, R. D. Porter, Y. K. Mo, D. P. Kelly and G. D. Mateescu, *J. Am. Chem. Soc.*, 1978, **100**, 6299.
19 M. Attina, F. Cacace and A. Ricci, *J. Am. Chem. Soc.*, 1991, **113**, 593.
20 T. Su and M. T. Bowers, in *Gas Phase Ion Chemistry*, ed. M. T. Bowers, Academic Press, New York, 1979, vol. 1, ch. 3.
21 M. T. Fernandez, K. R. Jennings and R. S. Mason, *J. Chem. Soc., Faraday Trans. 2*, 1989, **85**, 8513.
22 R. S. Mason, M. T. Fernandez and K. R. Jennings, *Adv. Mass Spectrom.*, 1985, **10**, 1167.
23 O. Exner, *Prog. Phys. Org. Chem.*, 1973, **10**, 411.
24 G. M. Roberts, *J. Org. Chem.*, 1982, **47**, 4050.
25 M. R. A. Falcini and K. R. Jennings, *Adv. Mass Spectrom.*, 1989, **11**, 552.

Paper 2/03207D; *Received* 18*th June*, 1992